

A Turbulent Friction and Heat Transfer Study of Dispersed Fluids with Ultra-Micronized Metallic Particles

Bock Choon Pak,* Seong Hoon Choi, Byung Joon Baek** and H. Masuda*****

(Received January 26, 1994)

Turbulent friction and heat transfer behaviors of dispersed fluids with ultra-micronized metallic particles are experimentally investigated in a circular pipe. Viscosity measurements are also conducted by using a viscometer. Aqueous mixtures with γ -Al₂O₃ and TiO₂ particles of which the mean diameters are 13 and 27 nm, respectively, are used to represent the dispersed fluids. The ranges of Reynolds and Prandtl numbers tested are 10⁴~10⁵ and 5.6~10.7, respectively. The relative viscosity of the dispersed fluid with γ -Al₂O₃ particles is about two hundred at the 10% volume concentration, while that of the dispersed fluid with TiO₂ particles is about twenty at the same volume concentration. Both of the relative viscosities are the unexpected results compared with predictions from classical theory of suspension rheology. Darcy friction factors for the comparatively dilute dispersion fluids used in present study coincide well with Kays correlation for turbulent flow of a single phase fluid, which implies that additional pumping power is not required despite adding solid particles into water. The Nusselt number of both the dispersed fluids for fully developed turbulent flow increases with increasing the volume concentration as well as the Reynolds number as expected. At the maximum volume concentration of 3% approximately, the percentage heat transfer enhancement due to addition of particles for the γ -Al₂O₃ and TiO₂ dispersing fluid systems are 60% and 30%, respectively. Under the range of volume concentration in the present study, the new correlation for turbulent convective heat transfer for both of the dispersed fluids is given by the following equation: $Nu = 0.021Re^{0.8}Pr^{0.5}$

Key Words : Viscosity, Heat Transfer Enhancement, Pressure Drop, Dispersed Fluid, Ultra-Micronized Metallic Particle

1. Introduction

Enhancement techniques in heat transfer technology have been attracted to researchers and engineers in response to the need for more efficient power and process heat exchanger, the appearance of commercial nuclear power, and the demand of space flight systems since the mid-

1950s. Furthermore, another significant increase in research activities stimulated by the 1973 oil crisis is evident from the exponential increase of the articles devoted to this subject so far. Among many articles, several recent review papers (Bergles, 1969, 1988; Nakayama, 1982) and handbook sections (Bergles, 1983, 1985) covering a variety of methods for augmenting heat transfer are available in the literature.

Generally, enhancement techniques can be categorized as passive and active methods depending on whether the additional external power is required or not (Bergles, 1985, 1988). The passive schemes, which require no direct application of the external power, include use of extended surfaces, swirl flow devices, additives for liquid and

*Department of Mech. Eng. and Design, Chonbuk National University, Chonju, Korea.

**Department of Precision Mech. Eng., Chonbuk National University, Chonju, Korea.

***Institute of fluid Science, Tohoku University, Sendai, Japan.

gases, while the active methods involve vibration of heated surface, vibration of fluid, injection or suction of fluid etc.. As one of the passive methods, some additives such as solid particles, gas bubbles, and phase change materials in single-phase flow and liquid trace additives for boiling systems are included in fluid. Especially, a new technique utilizing phase change materials in district cooling and thermal control systems has been also investigated (Kasza and Chen, 1982; Sengupta, 1989; Pak et al., 1989; Charunyakorn et al., 1991). In contrast, utilization of the solid particles as additive are rarely found (Ahuja, 1975, 1982; Shon, 1982, 1984) and were conducted in the laminar flow region only. Ahuja (1975) performed the experiments on augmentation of heat transport in laminar flow of polystyrene suspensions systematically. His experiments were based on overall heat transfer measurements in a shell and tube heat exchanger, employing the Graetz entrance flow conditions. The results showed that remarkable enhancements of Nusselt number and heat exchanger effectiveness were attainable when polystyrene spheres were added to a single-phase liquid. Sohn and Chen (1982) also reported the thermal conductivity of a dispersed two-phase mixture in a low velocity and Couette flow conditions, of which the results showed the thermal conductivity increases with increasing the shear rate when the particle Peclet number is sufficiently high.

On the other hand, a couple of studies (Yamada, 1989; Masud, 1993) have been performed recently in order to control the thermophysical properties of materials (continuous phases) by dispersing other materials (solid phases) having properties different from the continuous phase, that is, by using dispersed systems. Masuda et al. (1993) demonstrated the thermal conductivity of the mixtures of liquid and ultra-fine metallic particles (such as $\gamma\text{-Al}_2\text{O}_3$ and TiO_2) increased considerably by adding small amount of particles to single-phase suspending liquids. For water- $\gamma\text{-Al}_2\text{O}_3$ and water- TiO_2 particle mixtures, the amount of increase in the thermal conductivity were approximately 30% and 12% at the volume fraction of 4.3%, respectively. Hence, the

dispersed fluids might be used as fluid medium for convective heat transfer enhancement without excessive pressure drop penalties. In reality, this work stemmed from the study of effective thermal conductivity of aforementioned dispersed fluids.

To verify this concept in practical heat transfer problems, it is necessary to understand the fluid dynamics and heat transfer characteristics of these dispersed two-phase fluids in a straight pipe. The aim of the present study were to investigate the single-phase forced convection heat transfer characteristics of dispersed fluids with ultramicro-sized particles over the turbulent flow regime and viscosity as well.

2. Experimental Facility and Method

2.1 Experimental set-up and instrumentation

The schematic illustration of the flow loop built in a recirculation mode is shown in Fig. 1. The flow loop includes a 0.2 m^3 stainless steel reservoir tank, a pump, a by-pass line, a surge tank, a calming chamber, a hydrodynamic entry section, a heat transfer test section, a mixing chamber, and a fluid collection apparatus for measuring and calibrating flow rates. The hydrodynamic entry section and the heat transfer test section were fabricated using a seamless stainless steel tube (type 304), of which the inside diameter and the total length are 1.066 cm and 480 cm, respectively. The hydrodynamic entry section in the current study was long (i. e., $x/D = 157$) enough to accomplish fully developed flow at the entrance of the heat transfer test section. The remaining parts of the flow loop, except for the hydrodynamic entry and heat transfer test

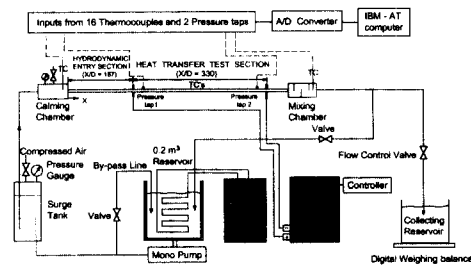


Fig. 1 Schematic diagram of the experimental set-up for pressure drop and heat transfer

section, were fabricated from welded stainless steel tube with an outer diameter of 2.52 cm.

A total of 14 thermocouples and two pressure taps were mounted along the heat transfer test section for temperature and pressure drop measurements, respectively. Especially, at two different locations, four thermocouples were installed circumferentially to check circumferential temperature variations during tests. To obtain a constant heat flux boundary condition, the heat transfer test section was heated electrically by a constant DC power supplier capable of delivering a maximum of 15 kW at a maximum of 15 V. To minimize parasitic heat loss due to axial heat conduction, the test section was isolated electrically and thermally from its upstream and downstream sections by Nylon bushings. To avoid convective heat loss to the surroundings, the heat transfer section, as well as the calming and mixing chambers, were wrapped with 7.6-cm-thick fiberglass insulation blankets. Also, a rapid chiller of which the cooling capability was 54,000 kJ/hr was utilized so that the inlet bulk temperature of the test fluids could be kept constant.

The essential quantity to be measured during a test was outer wall temperatures along the heat transfer test section at 14 different locations. Also measured were bulk temperatures, mass flow rates, electric power inputs, and pressure drops along the test section. In particular, the inlet and outlet bulk temperatures were measured in a calming chamber and in a mixing chamber, respectively.

The flow rate was controlled with two valves—one at the main flow loop and the other on a by-pass line (see Fig. 1). Flow rates were directly measured by weighing collected test fluids exiting from the outlet of the flow loop. A 2 m long flexible vinyl tubing was connected to the end of the flow loop in such a way that flow rate measurement procedure would not change flow rate itself, which would not be a trivial problem if one had used a three-way switching valve.

The pressure drop measurements were performed with a Validyne DP103-18 pressure transducer with 4 different diaphragms depending on the range of pressure to be measured. Prior to the

experiments, the pressure transducer was carefully calibrated with an inclined mercury manometer accurate to 0.5 mm Hg. Fourteen thermocouples (T-type) were cemented with a high thermal-conductivity-epoxy to the outside surface of the heat transfer test tube. The thermocouples were calibrated by ice point and steam point of distilled water before they were attached to the test section. All the temperature and pressure data were recorded directly into the IBM compatible PC through a 16-channel, 16-bit high resolution data acquisition system. It should be mentioned that, without heating the test section, the pressure drop measurements were proceeded to the heat transfer experiments to minimize the temperature effect on the viscosity of test fluids.

2.2 Dispersed fluids studied and property measurements

Ultra-Micronized γ - Al_2O_3 particles (Japan Aerosil Co. Ltd.) and TiO_2 particles (Titan Kogy, Japan) from several candidates were chosen as solid phase for the dispersed fluids used in the current study since it was comparatively easy to make the stable dispersed fluids with them. Distilled water was used for the suspending liquid medium. The mean diameters of γ - Al_2O_3 and TiO_2 particles are 13 and 27 nm, respectively. The other physical properties of particles are also shown in Table 1. As the photomicrographs of the ultra-fine particles used are shown in Fig. 2, both are irregular grain-like shapes with the axial ratio of unity approximately.

In order to prevent the solid particles from settling due to the density difference, a technique using the electrostatic repulsion forces between particle surfaces generated by adjustment of pH value was used, which will be summarized in the following briefly. In preparing dispersed fluids for a desired mass concentration, the required amount of particles weighed by a precision balance was mixed with the base fluid and the pH value was adjusted with extremely small amount of hydrochloric acid or sodium chloride depending on the type of particles. After stirring with a very high-speed mixer at the speed of 10,000 r.p.m. for a couple of hours, the dispersed fluid was allowed to set for several days. In order to deter-

Table 1 Physical properties of the ultra-micronized particles

Ultra-fine Particles	mean diameter* (nm)	Density (kg/m ³)	Specific surface ⁺ area(m ² /g)	Thermal conductivity (W/mK)
γ -Al ₂ O ₃	13	3880	100 ± 15	36
TiO ₂ (Anatase)	27	4175	56	8.4

*Data obtained from the manufactures.

⁺Data for 0~2% prosity, at 300 K.

mine the best pH value in making the homogeneous dispersion fluid, the procedure was repeated by varying the pH value. From a series of experiments, it was found that the mixed fluids with γ -Al₂O₃ and TiO₂ particles were dispersed homogeneously at the pH value of 3 and 10, respectively. Despite the difference in densities between the particles and the fluids it was observed no evidence of irreversible effects due to settling.

The viscosities of the dispersed fluids were measured by a Brookfield viscometer with cone-and-plate geometry, of which the fundamental principle and the overall procedure for measuring viscosity can be easily found elsewhere (Skelland, 1967, Barnes, 1989), over the wide range of shear rate. In order to examine the non-Newtonian behavior of viscosity, the experiments for each dispersed fluids were performed up to the maximum volume concentration of 10%. The densities were also measured by using various density-hydrometers having appropriate measuring range for each volume concentration.

3. Results and Discussion

3.1 Viscosity measurements of the dispersed fluids

In the investigation on the rheology of suspensions, one point worth stressing is that the volume concentraion, which is defined as the fraction of space of the total suspension occupied by the suspended material, is so important because the rheology depends to a great extent on the hydrodynamic forces which act on the surface of particles of aggregates of particles, generally irrespective of the particle density. Hence, the volume-per-volume fraction, and not the weight-per-weight fraction, is often used in defining concentration. However, it is not an easy task to make a dispersed liquid to the desired volume concentration exactly compared with making a dispersed liquid to the desired mass concentration. Therefore, in the present study, the volume fraction is determined from the mass fraction of the dispersed liquid by the following equation :

$$\Phi_v = \frac{1}{\frac{1}{\Phi_m} \frac{\rho_p}{\rho_w} + 1} \tag{1}$$

Once the volume fraction is determined, the density of the dispersed liquid can be also calculated as follows :

$$\rho = (1 - \Phi_v)\rho_w + \Phi_v\rho_p \tag{2}$$

Figure 3 given the comparison of the experimental values, which were measured by density-hydrometers at 25°C, with the ones calculated from Eq. (2) for the densities of the dispersed liquids at various volume concentrations. As shown in the Fig. 3, the maximum deviation is

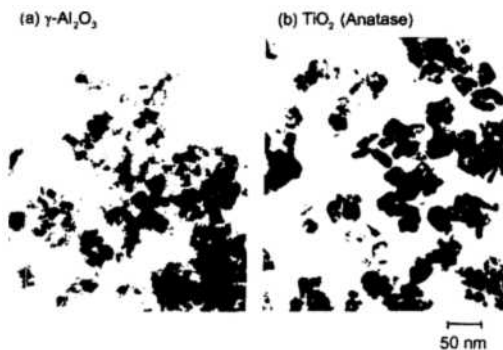


Fig. 2 Photomicrographs of ultra-fine metallic particles

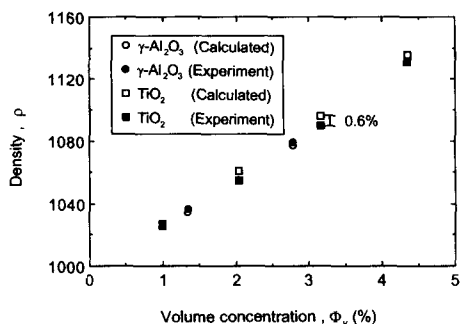


Fig. 3 Density vs. volume concentration of dispersed fluids

revealed only 0.6% at the volume fraction of 3.16%, from which the above-mentioned procedure may be validated.

The viscosity measurements of dispersed fluids with ultra-micronized metallic particles were conducted by a Brookfield viscometer (cone-and-plate type) with three different gap angles of 0.8, 1.565, and 3.0 degrees depending on the concentration of the test fluids. Prior to measuring the viscosities of the test fluids, calibration runs for the viscometer were preceded with distilled water and a standard sample fluid (4.3 mPa.s at 25°C) supplied by a manufacturer. Also, the viscosity measurements of the same test fluids with three different pH values, i. e., 3, 6 and 12, were conducted to examine the possible effect on the viscosity by adding small amount of hydrochloric acid or sodium chloride in preparation or the dispersed fluids. All the experiments were carried out at a constant temperature of 25°C. In the Fig. 4, the experimental results for the viscosities of water and a standard test sample, of which the average deviation is only 2% for all the calibration runs, agree well with the data in the literature and furnished by a manufacturer, respectively. Figure 4 also shows the influence of pH value on viscosity. Ippolito (1980) reported the influence of sodium chloride additions on the viscosity of aqueous bentonite suspensions. From his experiments, it was found that flocculated systems usually had very high viscosities at low shear rate, and were very shear thinning, often giving the impression of a yield stress. However, the current experimental results, as shown in Fig. 4, reveal no

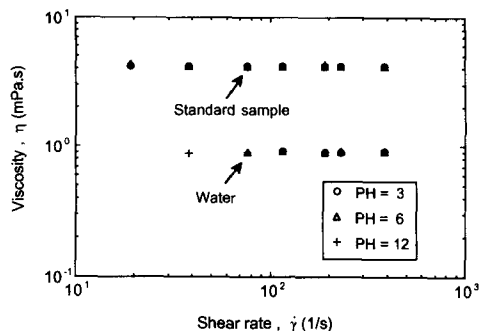


Fig. 4 Calibration runs for a viscometer and the pH effects on viscosity

influence of pH value on the viscosity of single phase fluids, which may be attributed to extremely small amount of hydrochloric acid or sodium chloride addition when being adjusted the pH value of test fluids.

The viscosities of two different kinds of dispersed fluids used in the current study are presented in Figs. 5~9. As mentioned earlier, the viscosity measurements were covered to the maximum volume concentration of 10% with approximately 1% increment over a wide range of shear rates. The effects of volume concentration on viscosity are shown in Figs. 5 and 6 for γ -Al₂O₃ and TiO₂ dispersing fluid systems, respectively and representatively. It should be noted that the range of shear rates for volume concentration were different from each other due to limitation of measuring capability of a viscometer. The viscosities of both dispersed fluids increase with increasing volume concentration as expected. Also, the shear-thinning behavior of the viscosity of the dispersed liquid with γ -Al₂O₃ particles begins to be observed at 3% volume concentration approximately, while that of the dispersed liquid with TiO₂ particles at 9%. Both cases are getting more apparently shown with increasing phase volume fraction.

Viscosity data used in Figs. 5~6 are replotted in Fig. 7 to represent the relative viscosity vs. volume concentration. Relative viscosity is usually defined as the ratio of viscosity of the filled fluid with suspensions to that of the unfilled fluid at the same shear rate. In case of the dispersed fluid with TiO₂ particles shown in Fig. 7, the

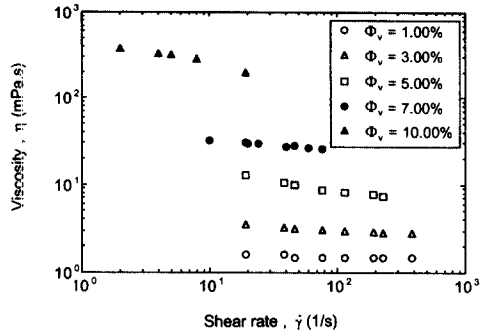


Fig. 5 Viscosity vs. shear rate for the dispersed fluids with $\gamma\text{-Al}_2\text{O}_3$ particles at different volume concentrations

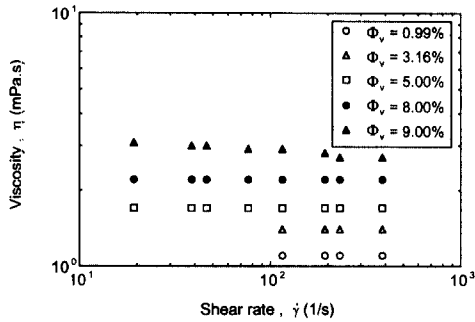


Fig. 6 Viscosity vs. shear rate for the dispersed fluids with TiO_2 particles at different volume concentrations

relative viscosity of 10% volume concentration, for example, is approximately twenty while that of the disperse system with $\gamma\text{-Al}_2\text{O}_3$ particles at the same volume fraction is about two hundreds, both of which are dramatic increases compared with the prediction values from an analytical theory by Bacheor(1977) for dilute fluid dispersed with solid spheres. Bachelor gives the viscosity in this case as follows

$$\eta_r = 1 + 2.5\Phi_v + 6.2\Phi_v^2 \quad (3)$$

where this equation covers the range below 10% volume phase. Note that a number of experimental determinations of the coefficient of Φ_v^2 term for shear flows have been made, but the range of values so obtained is varying from about 5 to 15, which accounts for no more than a 40% increase in viscosity over the continuous phase. However, it was pointed out by Rutgers(1962) that sphere size

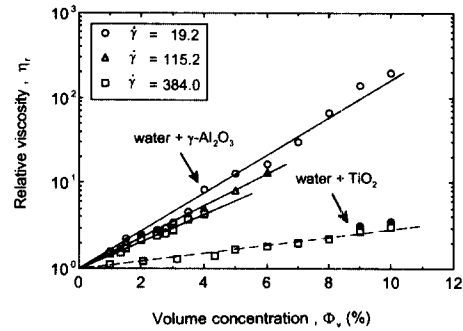


Fig. 7 Relative viscosity vs. volume concentration at different shear rates

should have an influence, i. e. smaller diameter below about $0.5 \mu\text{m}$ causing always higher relative viscosity. In the present study, such a surprising increase in viscosity of the disperse fluids may be attributed primarily to the extremely small size of particles, from which arises strong interactions between the particles, and secondly to the irregular shape of the particles with a rough surface, resulting in the increase of specific surface area. Figure 7 also shows that relative viscosity increases with decreasing shear rate at a constant volume concentration in the case of the disperse fluid with $\gamma\text{-Al}_2\text{O}_3$ particles, especially. The results qualitatively agree well with the previous experimental investigations(Krieger, 1972, de Kruif et al., 1985) which present the ultimate shear-rate, i. e., zero shear rate and infinite shear rate, asymptotic values of relative viscosity versus phase volume for monodisperse lattices.

Figures 8 and 9 present the temperature-dependent behavior of viscosity for $\gamma\text{-Al}_2\text{O}_3$ and TiO_2 dispersing fluid systems, respectively. The corresponding curves for pure water are shown as solid lines in the figures for an easy comparison. As expected, the viscosities of dispersed fluid systems decrease exponentially with increasing temperature, while increase with increasing volume fraction. It should be mentioned that the exponential curve fittings for temperature-dependent viscosity for each volume concentration were used for data reduction procedure in pressure drop and heat transfer experiments to take the temperature effect on viscosity into

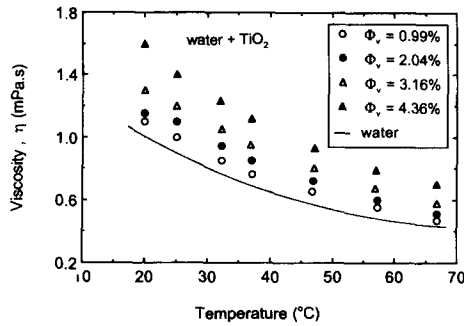


Fig. 8 Temperature effects on viscosity of the dispersed fluids with $\gamma\text{-Al}_2\text{O}_3$ particles

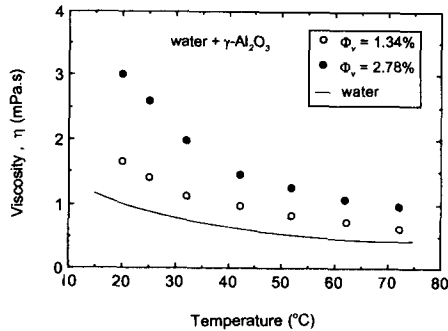


Fig. 9 Temperature effects on viscosity of the dispersed fluids with TiO_2 particles

account.

3.2 Pressure drop and heat transfer experiments

Before the experiments with dispersed fluids, system calibration tests are carried out with distilled water to check the validity of the experimental apparatus and overall experimental procedure. First, accuracy tests in heat transfer measurements are carried out by comparing the electric energy supplied to the stainless steel tube with the thermal energy removed by the fluid under the condition of no parasitic heat loss. The energy balance ratio, E. B. R., is defined as

$$\text{E. B. R.} =$$

$$\frac{\text{Thermal energy removed by the fluid}}{\text{Electric energy supplied by the power supply}}$$

The energy balance ratios, as shown in Fig. 10, are calculated by measuring the bulk mean temperatures of water at the inlet and outlet of the test section and the voltage drop and current over

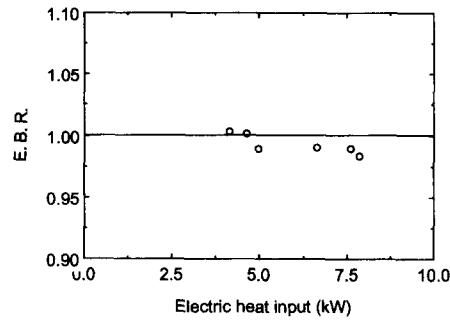


Fig. 10 Energy balance ratio (EBR) of the heating system

the test section. The energy balance ratios are within approximately 2% of unity. Uniform heat flux condition is also ensured by comparing the temperatures at 8 points with an equal angle circumferentially at two locations ($x/D=105$ and 210) along the test section. Several measurements at different Reynolds number and heat input show that circumferential temperature variations of the test tube are negligibly small, however, not shown in the present paper.

The accuracy of the pressure measuring system is checked by circulating distilled water without heating and measuring pressure drop along the test section, from which the Darcy friction factors are calculated and compared with the Blasius resistance formula (Schlichting, 1979) and the correlations recommended by Kays (1993) as follows:

$$\text{Blasius: } f = 0.316 Re^{-0.25} \quad 5 \times 10^3 < Re < 3 \times 10^4 \quad (4)$$

$$\text{Kays: } f = 0.312 Re^{-0.25} \quad 5 \times 10^3 < Re < 3 \times 10^4$$

$$f = 0.184 Re^{-0.2} \quad 3 \times 10^4 < Re < 10^6 \quad (5)$$

Tests are conducted with water at various Reynolds number, and the measured Darcy friction coefficients are shown in the upper part of Fig. 11. The maximum deviation of the measured Darcy friction coefficients from the predicted values with Kays' correlation was 2% over the range of the Reynolds number.

The accuracy of the temperature measuring system is tested by comparing the measured

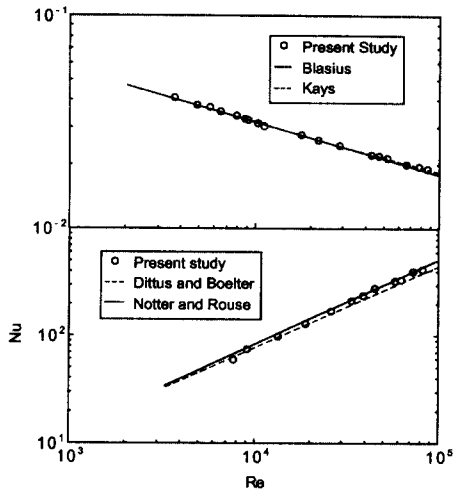


Fig. 11 Comparison of measured Darcy friction coefficients and Nusselt numbers with the predicted values from previous correlations for water

Nusselt numbers at the fully developed region of the test section to the predicted values from Dittus-Boelter(1930) and Notter-Rouse equations(1972). The Dittus-Boelter equation for turbulent flow is given as

$$Nu = 0.023 Re^{0.8} Pr^{0.4} \quad (6)$$

The Notter-Rouse correlation is also given as

$$Nu = 5 + 0.015 Re^{0.856} Pr^{0.347} \quad (7)$$

Experimentally, the convective heat transfer coefficient and the corresponding Nusselt number for the fully developed turbulent flow are calculated as

$$h = \dot{q} / (T_w - T_b) \quad (8)$$

$$Nu = hD / k_f \quad (9)$$

More detailed information for data reduction procedure can be found elsewhere(Pak ; 1991). The small temperature difference between inlet and outlet, as well as between wall and bulk temperatures, is important in minimizing the effect of temperature-dependent viscosity on the calculation of the overall heat transfer coefficient. The maximum temperature difference between the inlet temperature of the test fluids and the inner wall temperature at the exit is less than 8°C for all runs. The local Reynolds and Prandtl numbers

are calculated with the thermophysical properties based on the local bulk mean temperature. The Nusselt number is determined by averaging the local Nusselt numbers in the thermally fully developed region over the heat transfer test section. As shown in the lower part of Fig. 11, the measured Nusselt numbers for water is between the two values predicted by the previous correlations(Dittus and Boelter, 1930 ; Notter and Rouse, 1972). It should be noted that the dispersed fluids with comparatively dilute concentrations(i. e. less than 3%) were used in pressure drop and heat transfer measurements from practical point of view. Also, note that the thermal conductivity data of the dispersed fluids obtained by the previous experiments(Masuda, 1993) were used for heat transfer data reduction.

Figure 12 presents the Darcy friction coefficients as a function of the Reynolds number for the dilute dispersion fluids with ultra-fine γ -Al₂O₃ and TiO₂ particles. Kays correlation for turbulent flow of a single phase fluid is inserted as a solid line to facilitate comparison. As shown in the figure, the friction coefficients for dispersed fluids coincide well with Kays' predictions regardless of the volume concentration, which implies that additional pumping power is not required in spite of adding solid particles into water. The deviation from the predicted values with Kays correlation is within 3% over the range of Reynolds number in the present experiments. It may be noted that the pressure drop is independent of the particle size(seen for 13 and 27 nm particles) as long as volume concentration is low. Ahuja(1975) report-

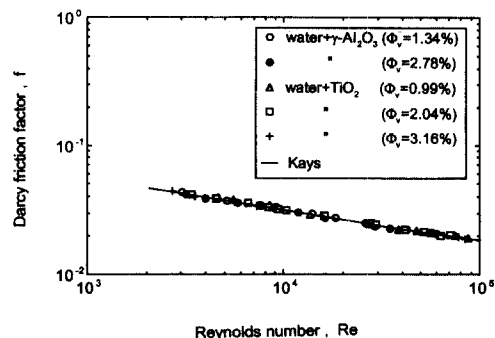


Fig. 12 Darcy friction coefficients of dispersed fluids

ed that the friction factor for 20% volume concentration is about 7.5 less than the one corresponding to Poiseuille flow in laminar flow of polystyrene suspensions of $50\ \mu\text{m}$ in diameter, which is due to the so-called σ phenomenon (Goldsmith and Mason, 1967). However, the present results showing no decrement in friction factor may be explained by the fact that the volume concentration is pretty low and, moreover, the flow is turbulent.

Turbulent heat transfer results for dilutely dispersed fluids with the same volume fractions as the pressure drop measurements are presented in Fig. 13. The upper part of Fig. 13 indicates the Nusselt number versus the Reynolds number for $\gamma\text{-Al}_2\text{O}_3$ dispersion fluids contrary to the lower part of the figure for TiO_2 dispersion fluids. In both figures, Dittus-Boelter correlation for single-phase fluid, i. e., zero concentration dispersion fluid, is inserted with a solid line for reference. As shown in the upper figure, the Nusselt number increases with increasing the Reynolds number and the volume concentration as well. Under the constant Reynolds number, heat transfer enhance-

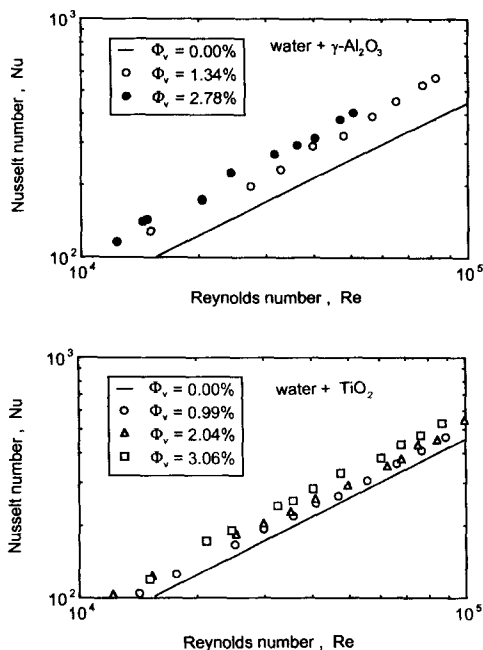


Fig. 13 Nusselt number vs. Reynolds number for dispersed fluids.

ment due to addition of ultra-fine $\gamma\text{-Al}_2\text{O}_3$ particles is about 35 percent for the volume fraction of 1.34% and about 60 percent for that of 2.78%, respectively. A similar trend in heat transfer enhancement for TiO_2 dispersion fluids is also observed as shown in the lower part of Fig. 13. However, the major difference between those two dispersed fluids is the fact that the degree of heat transfer enhancement for TiO_2 dispersion fluid is lower than that for $\gamma\text{-Al}_2\text{O}_3$ dispersion fluid although it cannot be compared accurately due to the different concentration of the two. It is interesting to note that the 0.8 exponent of the Reynolds number occurs in a wide range of physical situations involving turbulent flows. In Fig. 14, the Nusselt numbers are brought as a function of the Prandtl number instead of volume concentration and the Reynolds number with the 0.8 exponent, together. The new correlation is shown as a solid line in Fig. 14 and can be shown by the following relationship:

$$Nu = 0.021 Re^{0.8} Pr^{0.5} \quad (10)$$

This correlation was obtained by curve-fitting all the data of dispersed fluids including water.

Note that the maximum deviation in the curve-fitting was 4.8% and the ranges of Reynolds and Prandtl numbers tested were $10^4 \sim 10^5$ and 5.6 \sim 10.7, respectively. From this empirical correlation, it is clear that the Nusselt number for the dispersed fluids is slightly more dependent on the Prandtl number when compared with that for single-phase fluid. Conclusively, it is said that the dispersion fluids added by small amount of ultra-

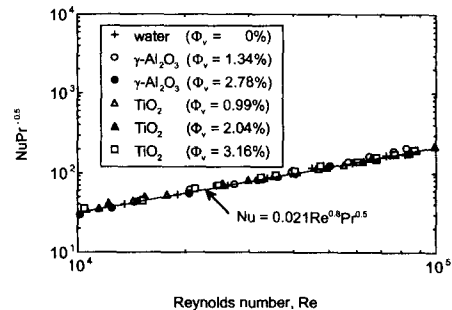


Fig. 14 Dimensionless representation of heat transfer measurements for dispersed fluids

fine particles may be utilized as a working medium, without pumping loss, to enhance heat transfer performance in heat transfer processes of many energy-intensive industries.

4. Summary and conclusions

Turbulent friction and heat transfer behaviors of dispersed fluids with ultra-micronized $\gamma\text{-Al}_2\text{O}_3$ and TiO_2 particles are experimentally investigated in a circular pipe. Viscosity measurements of those fluids are also conducted by using a viscometer. Important findings are briefly summarized below.

(1) The shear thinning behavior of viscosity for the dispersed fluids with $\gamma\text{-Al}_2\text{O}_3$ and TiO_2 particles is observed at the volume concentration of 3% and 9%, respectively, and is shown more apparently by increase of volume concentration.

(2) At the 10% volume concentration, the relative viscosity for the dispersed fluid with $\gamma\text{-Al}_2\text{O}_3$ particles is about two hundred while it is about twenty for dispersed fluids with TiO_2 particles, which are the unexpected results compared with predictions from classical theory of suspension rheology. From the measurements, it is believed that the size of solid particle in dispersed fluid systems plays a significant role on viscosity at the sub-micron level, especially.

(3) Darcy friction factors for the comparatively dilute dispersion fluids used in present study coincide well with Kays' correlation for turbulent flow of a single phase fluid, which implies that no additional pumping power is required in spite of adding solid particles into water.

(4) The Nusselt number for the dispersed fluids increases with increasing volume concentration as well as the Reynolds number, as expected. At the maximum volume concentration of approximately 3%, the percentage heat transfer enhancement due to addition of particles for the $\gamma\text{-Al}_2\text{O}_3$ and TiO_2 dispersing fluid systems are 60% and 30%, respectively. Under the experimental ranges of volume concentration (0~3%), the Reynolds number ($10^4 \sim 10^5$) and the Prandtl number (5.6~10.7) in the present study, the new correlation for the dispersed fluids is suggested as $Nu = 0.021 Re^{0.8} Pr^{0.8}$.

Acknowledgement

The authors acknowledge the financial support of Korea Research Foundation in 1992. In addition, the authors wish to express appreciation to Japan Aerosil Co. Ltd. and Titan Kogyo, Japan for supply of the experimental materials.

References

- Ahuja, A. S., 1975, "Augmentation of Heat Transport in Laminar Flow of Polystyrene Suspensions. I. Experiments and Results," *J. Applied Physics*, Vol. 46, No. 8, pp. 3408~3416.
- Ahuja, A. S., 1982, "Thermal Design of a Heat Exchanger Employing Laminar Flow of Particle Suspensions," *Int. J. Heat and Mass Transfer*, Vol. 25, No. 5, pp. 725~728.
- Barnes, H. A., Hutton, J. F. and Walters, K., 1989, *An Introduction to Rheology*, Elsevier Sci. Publishers B. V., pp. 25~35.
- Bergles, A. E., 1969, "Survey and Evaluation of Techniques to Augment Convective Heat and Mass Transfer," in *Progress in Heat and Mass Transfer* (Edited by U. Grigull and E. Hahne). Vol. 1, Pergamon Press, New York, pp. 331~424.
- Bergles, A. E., 1983, "Augmentation of Heat Transfer," *Heat Exchanger Design Handbook*, Vol. 2, Hemisphere Publishing Corp., Washing, D. D., pp. 2.5.11-1-12.
- Bergles, A. E., 1985, "Techniques to Augment Heat Transfer," *Handbook of Heat Transfer Applications*, McGraw-Hill, New York, NY, pp. 3-1-80.
- Bergles, A. E., 1988, "Some Perspectives on Enhanced Heat Transfer-Second-Generation Heat Transfer Technology," *ASME Trans. J. of Heat Transfer*, Vol. 110, pp. 1082~1096.
- Charunyakorn, P., Sengupta, S. and Roy, S. K., 1991, "Forced Convection Heat Transfer in Microencapsulated Phase Change Material Slurries: Flow in Circular Ducts," *Int. J. of Heat and Mass Transfer*, Vol. 34, No. 3, pp. 819~833.
- de Kruijff, C. G., van Ievsel, E. M. F., Vrij, A. and Russel, W. B., 1985, "Hard Sphere Colloidal Dispersions: Viscosity as a Function of Shear

Rate and Volume Fraction," J. Chemical Physics, Vol. 83, pp. 4717~4725.

Dittus, F. W. and Boelter, L. M. K., 1930, "Heat Transfer in Automobile Radiators of the Tubular Type," Univ. Calif. Publ. in Eng., Vol. 11, pp. 443~461.

Goldsmith, H. L. and Mason, S. G., 1967, "Rheology: Theory and Applications," Vol. 4, Chap. 2, Edited by Eirich F. R., Academic Press, New York.

Ippolito, M., 1980, "Rheology of Dispersed Systems-Influence of NaCl on the Viscous Properties of Aqueous Bentonite Suspensions," in Rheology, Vol. 2: Fluids, Edited by G. Astarita et al., Plenum Press, pp. 651~658.

Kasza, K. E. and Chen, M. M., 1982, "Development of Enhanced Heat Transfer/Transport/Storage Slurries for Thermal-System Improvement," Argonne Nat. Lab., ANL-82-50.

Kays, W. M. and Crawford, M. E., 1993, Convective Heat and Mass Transfer, 3rd Ed., McGraw-Hill, pp. 244~249.

Krieger, I. M., 1972, "Rheology of Monodisperse Latices," Adv. Colloid Interface Science, Vol. 3, pp. 111~136.

Masuda, H., Ebata, A., Teramae, K. and Hishinuma, N., 1993, "Alteration of Thermal Conductivity and Viscosity of Liquid by Dispersing Ultra-Fine Particles (Dispersion of γ -Al₂O₃, SiO₂ and TiO₂ Ultra-Fine Particles)," Netsu Bussei (Japan), Vol. 4, No. 4, pp. 227~233.

Nakayama, W., 1982, "Enhancement of Heat Transfer," Heat Transfer 1982, Proceedings, 7th International Heat Transfer Conference, Hemisphere Publishing Corp., Washing, D. C., Vol. pp. 223~240.

Notter, R. H. and Rouse, M. W., 1972, "A Solution to the Turbulent Graetz Problem-III.

Fully Developed Region Heat Transfer Rates," Chem. Eng. Sci., Vol. 27, pp. 2073~2093.

Pak, B. C., Choi, Y. I. and Lorsh, H., 1989, "Use of Advanced Low Temperature Heat Transfer Fluid for District Cooling System," Int. District Heating and Cooling System Conference at Virginia Beach, June 21-24, No. 269, Vol. 85, pp. 368~376.

Pak, B. C., Cho, Y. I. and Choi, Stephen U. S., 1991, "A Study of Turbulent Heat Transfer in a Sudden-Expansion Pipe with Drag-Reducing Viscoelastic Fluid," Int. J. of Heat and Mass Transfer, Vol. 34, No. 4/5, pp. 1195~1208.

Rutgers, Ir. R., 1962, "Relative Viscosity and Concentration," Rheologica Acta, Vol. 2, pp. 305~438.

Schlichting, H., 1979, Boundary Layer Theory, 7th Ed., McGraw-Hill, pp. 596~600.

Sengupta, S., 1989, "Microencapsulated Phase Change Material Slurries for Thermal Management of Electronic Package," Final Report, The Florida High Technology and Industry Council.

Shon, C. W. and Chen, M. M., 1984, "Microconvective Thermal Conductivity in Disperse Two-Phase Mixture as Observed in a Laminar Flow," ASME Trans., J. of Heat Transfer, Vol. 104, pp. 47~51.

Shon, C. W. and Chen, M. M., 1984, "Heat Transfer Enhancement in Laminar Slurry Pipe Flows with Power Law Thermal Conductive," ASME Trans., J. of Heat Transfer, Vol. 106, pp. 539~542.

Skelland, A. H. P., 1967, Non-Newtonian Flow and Heat Transfer, Chap. 2, Wiley, New York.

Yamada, E., 1989, "The Effective Thermal Conductivity of Dispersed materials," Japan J. of Thermo-Phys. Proper., Vol. 3, No. 2, pp. 78~83.